esophageal lumen. With rapidly evolving ablation technologies, these data support further study to reduce inadvertent injury to juxtaposed tissue, improve safety, and enhance efficiency.

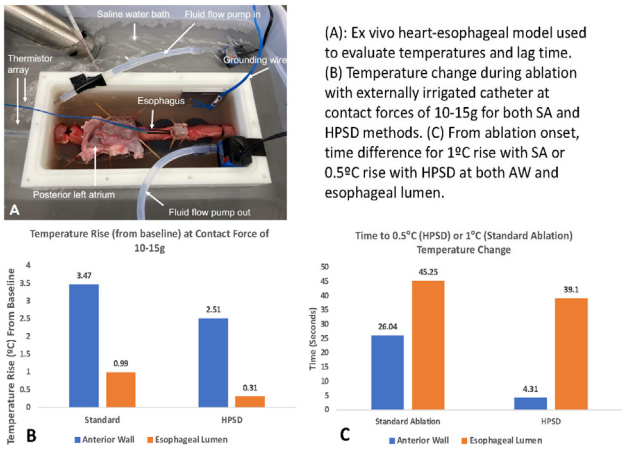

(A): Ex vivo heart-esophageal model used to evaluate temperatures and lag time. (B) Temperature change during ablation with externally irrigated catheter at contact forces of 10-15g for both SA and HPSD methods. (C) From ablation onset, time difference for 1ºC rise with SA or 0.5ºC rise with HPSD at both AW and esophageal lumen.

ABSTRACT CE-520:
Novel Arrhythmia Insights and Mapping Techniques

Friday, April 29, 2022
9:15 AM - 10:15 AM

CE-520-01

PULMONARY VEIN MYOCARDIAL SLEEVES ACT AS AMPLIFIER SITES DURING PERSISTENT ATRIAL FIBRILLATION: A HIGH DENSITY PHASE MAPPING STUDY

Ahmed Al-Kaisey MBChB; shu meng; Ramanathan Parameswaran MBBS; Robert Anderson MBBS; Joshua Hawson; Troy M. Watts BS, CCDS; David Budgett BENG; Bruce H. Smaill PhD and Jonathan M. Kalman MBBS, PhD, FHRS

Background: The mechanisms underlying persistent AF (PeAF) remain poorly defined. Although the substrate is not limited to the pulmonary veins (PVs), PV isolation (PVI) remains the best ablation strategy in PeAF.
Objective: To characterise the mechanisms of electrical activity originating in the PV sleeves during PeAF.
Methods: Eleven patients presenting for first time ablation for PeAF were recruited (63.1 ± 10.9 years, 91% males). Prior to PVI, a 64 electrode catheter (Constellation™; 38 mm) was introduced into the left atrium (LA) via trans septal access and positioned within the PV including the antral region under fluoroscopic guidance. A robust inverse mapping technique was used to reconstruct unipolar atrial EGMs on the PV surface and the resulting phase maps were used to identify incoming and outgoing wavefronts (WF) at the PV junction (reentry), and focal and rotor activity originating within the PV sleeves. These events were overlaid on phase entropy-time plots that reflect activation and repolarization heterogeneity across the PV surface. Data were analysed over 10 secs periods and are presented as median [LQ; UQ] or mean±SD, if normally distributed.
Results: During PeAF, the PVs gave rise to outgoing WF with frequency 3.7Hz [3.4; 5.4]. The most common mechanism generating outgoing WF was circuitous macroscopic reentry where an incoming WF generated one or more outgoing WF (frequency of reentry 2.7Hz [1.9; 3.3] compared with focal activity 1.4Hz [1.05; 1.5] ($p<0.001$). Rotors within the PV sleeve were rarely observed. Reentrant delay (time from wave-front entering to time of reentrant exit from the PV sleeve) was remarkably consistent between patients (125±46ms, range 30-260 ms, n=282). Higher outgoing frequencies were associated with repeated cycles of reentry (1 incoming wave generating 2 or more reentrant outgoing WF) and elevated phase entropy ($R^2 = 0.94$ and 0.93, respectively, $p<0.001$). The median ratio of incoming to outgoing PV activity was 1.14 (LQ=0.84, UQ=1.88). In 6/11 PVs (55%) the R was >1 (Mean 1.77±0.54, maximum 2.68).
Conclusion: Electrical activity generated by PV sleeves during PeAF is due mainly to macroscopic reentry initiated by incoming waves, frequently with a ratio>1. That is, the PVs act less as AF drivers than as “echo chambers” which sustain and amplify fibrillatory activity.

CE-520-02

ELECTRO-ANATOMIC REPOLARIZATION MAPPING WITH ORTHOGONAL BIPOLES AND MULTI-ELECTRODE ARRAYS: THE NEXT FRONTIER IN CATHETER TECHNOLOGY

Stephane Masse MASC, PE; Ahmed Niri BENG; John Asta; Mohammed Ali Azam; Patrick F.H. Lai MSci; Karl Magtibay BENG, MASC; D. Curtis Deno MD, PhD and Kumaraswamy Nanthakumar MD

Background: Sites of steep repolarization gradients have been attributed to arrhythmogenesis. However, identifying these regions during clinical mapping has not materialized. Activation interval recovery (ARI), monophasic action potential (MAP) and optical mapping are not practical for clinical usage during ablation procedure. Clinical repolarization mapping has not been practically viable largely due to instrumentation and signal processing challenges. We developed here a repolarization mapping technology from orthogonal bipole derived vector loops in multielectrode array and the time projection of the repolarization loop electrogram (loop derived repolarization-optimized egm, (rEGM), for assessment of repolarization on mapping arrays.
Objective: We hypothesised that rEGM provides vector derived integrated action potential duration (APD^V) that correlates with local repolarization assessed by optical mapping.
Methods: Simultaneous optical mapping and epicardial mapping with Abbott Advisor™ HD Grid was performed in 4 rabbit Langendorff experiments. Unipolar egms from 4 electrodes forming a square in the middle of the grid were recorded and intra-cardiac vectorcardiogram loops computed from orthogonal derived bipoles. rEGM was obtained by projecting the repolarization loop along its maximum axis. Epicardial waves propagating in different direction and pinacidil was added to alter APD. APD^V was measured from the onset of QRS to baseline return of rEGM. rEGM derived APD^V were compared with fluorescence signals and optical APD90 measured in the middle of the electrode clique.
Results: A total of 61 pairs of APD^V measurements were performed. Baseline conditions showed an VAPD average of 142ms versus APD90 of 151ms. After 20uM addition of pinacidil ARI and APD were reduced to 68ms and 89ms respectively. Linear correlation between APD^V and APD90 showed a R^2 of 0.7134 and a slope of 0.9540.
Conclusion: These results suggests that multi-electrode arrays with orthogonal bipoles could provide intra-electrode cardiac vector loops that enable local APD measurements for mapping utility. This concept ushers an era of using multi-electrode arrays to perform repolarization mapping and create 3D electro-anatomic repolarization maps to identify regions of steep repolarization gradients.

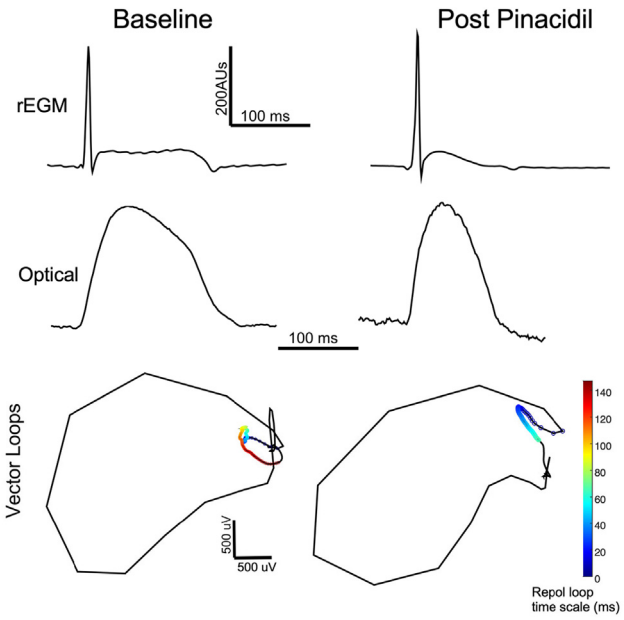

Figure 1. Illustrative example of rEGMs and associated voltage loops shown with fluorescence signals.
A: rEGM at baseline (left) and after pinacidil infuson (right).
B: Optical signals measured at same locations.
C: Vector loops obtained from orthogonal bipoles. Large component traced in black represents the QRS while the color coded segment illustrates the repolarization loop. Color depicts time of repolarization.

CE-520-03

USE OF RIPPLE MAPPING TO ENHANCE LOCALIZATION AND ABLATION OF OUTFLOW TRACT PREMATURE VENTRICULAR CONTRACTIONS

Kelly Arps MD; Adam S. Barnett MD; Jason I. Koontz MD, PhD; Sean D. Pokorney MD, MBA; Kevin P. Jackson MD; Tristram D. Bahnson MD, FHRS; Jonathan P. Piccini MD, MHS, FHRS and Albert Y. Sun MD

Background: Mapping outflow tract (OT) premature ventricular contractions (PVCs) can be difficult given a frequent mid-myocardial origin. Compared to local activation time mapping, Carto® Ripple Mapping provides visualization of both far field and near field signals independent of local annotation that may enhance PVC localization.
Objective: To evaluate the utility of Ripple mapping to localize OT PVCs.
Methods: Electroanatomic maps for consecutive OT PVC catheter ablation cases (July 2018-December 2020) were analyzed. For each PVC, we identified the earliest local activation point (EA), defined by the point of maximal -dV/dt in the unipolar electrogram (EGM) within each corresponding bipolar EGM, and the earliest Ripple signal (ERS), defined as the earliest point at which 3 grouped simultaneous Ripple bars appeared. Procedural success was defined as full suppression of the targeted PVC.
Results: 57 PVC maps were included. When ERS was in the same chamber (right ventricle, left ventricle, or coronary sinus) as EA, procedural success was 84%, versus 29% when discordant ($p < 0.01$) (Figure). Site discordance had an odds ratio for needing multisite ablation of 7.9 (95% confidence interval 1.4-4.6; $p = 0.02$) and for unsuccessful procedure of 13.1 (2.2-79.9; $p<0.01$). Median EA-ERS distance in successful and unsuccessful cases was 4.6 mm (interquartile range 2.9, 8.5) vs 12.5 mm (7.8, 18.5); ($p<0.01$). Positive predictive value for successful ablation with EA-ERS distance <10mm was 90% (79-95%, $p<0.01$).
Conclusion: Greater concordance between EA and ERS is associated with higher odds of successful OT PVC ablation. Visualization of far-field signals via Ripple mapping may offer localization information complementary to activation mapping for PVCs of mid-myocardial origin.

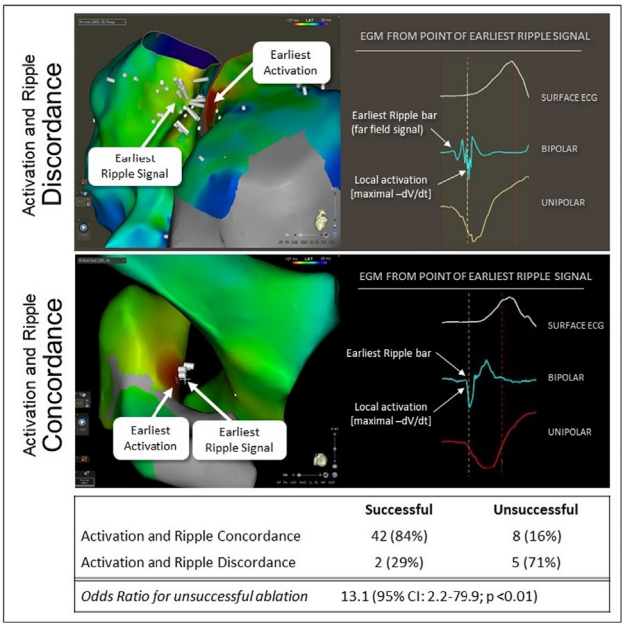

	Successful	Unsuccessful
Activation and Ripple Concordance	42 (84%)	8 (16%)
Activation and Ripple Discordance	2 (29%)	5 (71%)
Odds Ratio for unsuccessful ablation	13.1 (95% CI: 2.2-79.9; p <0.01)	

CE-520-04

FORWARD-SOLUTION COMPUTATIONAL ARRHYTHMIA SOURCE MAPPING: THE VMAP STUDY

David E. Krummen MD; Christopher T. Villongco PhD; Gordon Ho MD; Amir A. Schricker MD; Michael E. Field MD; Kevin Sung MD, MS; Katherine A. Kacena PhD; Melissa S. Martnson PhD, MS; Kurt S. Hoffmayer MD, PharmD; Jonathan C. Hsu MD, MAS; Farshad Raissi Shabari MD, MPH; Gregory K. Feld MD; Andrew D. McCulloch PhD and Frederick T. Han MD

Background: The accuracy of arrhythmia source localization using a forward solution computational mapping system has not yet been evaluated in blinded, multicenter analysis.
Objective: The study tested the hypothesis that a computational mapping system using a comprehensive arrhythmia simulation library would provide accurate localization of the site of origin for atrial and ventricular arrhythmias and pacing using the 12-lead ECG compared with the gold standard of invasive electrophysiology study and ablation.
Methods: The VMAP study was a blinded, multicenter evaluation with final data analysis performed by an independent core laboratory. Eligible episodes included atrial and ventricular: tachycardia (VT), fibrillation, pacing, premature complexes (PACs and PVCs; figure panel A); and orthodromic atrioventricular reentrant tachycardia. Forward solution mapping system results (panel B) were compared with the gold standard site of successful ablation or pacing during invasive electrophysiology study and ablation (panel C). Mapping time performance was assessed from timestamped analysis logs. Pre-specified performance goals were used for statistical comparisons.
Results: A total of 255 episodes from 225 patients were enrolled from 4 study centers. Regional accuracy for VT and PVCs in patients without significant structural heart disease (n=75,